

Superconductivity induced by Pd-doping in $\text{SrFe}_{2-x}\text{Pd}_x\text{As}_2$

Xiyu Zhu, Fei Han, Peng Cheng, Bing Shen and Hai-Hu Wen*

National Laboratory for Superconductivity, Institute of Physics and Beijing National Laboratory for Condensed Matter Physics, Chinese Academy of Sciences, P. O. Box 603, Beijing 100190, China

By using solid state reaction method, we have synthesized the Pd-doped superconductor $\text{SrFe}_{2-x}\text{Pd}_x\text{As}_2$. The systematic evolution of the lattice constants indicated that the Fe ions were successfully replaced by the Pd. By increasing the doping content of Pd, the antiferromagnetic order of the parent phase is suppressed and superconductivity is induced at a doping level of about $x=0.05$. Superconductivity with a maximum transition temperature T_c of about 8.7 K was achieved at a doping level of $x = 0.15$. The general phase diagram of T_c versus x was obtained and found to be similar to the case of Ni and Co doping to the Fe sites. Our results suggest that superconductivity can be easily induced in the FeAs family by adding charges into the system, regardless with the transition metals of 3d or higher d-orbital electrons.

PACS numbers: 74.70.Dd, 74.25.Fy, 75.30.Fv, 74.10.+v

Superconductivity in the FeAs-based systems has received tremendous attention since last year with the hope that the superconducting transition temperature could be raised to a higher value¹. The superconducting transition temperature was promoted above 50 K by replacing lanthanum with other rare-earth elements in $\text{LaFeAsO}^{2,3}$, or by substituting the alkaline elements with rare earth elements in $(\text{Ba},\text{Sr},\text{Ca})\text{FeAsF}^{4,5}$. Meanwhile, the hole-doped superconductors were discovered both in the FeAs-1111 and the FeAs-122 family^{6,7,8}. The FeAs-122 phase, due to the much simpler structure, less elements in the compound and easy growth of large scale single crystals, provides us a great opportunity to investigate the intrinsic physical properties^{9,10}. Meanwhile, people found that a substitution of Fe ions with Co or Ni can also induce superconductivity with the maximum T_c above 20 K^{11,12,13}. These early experiments were focused on the substitution of Fe ions with 3d-transition metals nearby Fe. Very recently, Ru and Ir substitution at Fe sites in the FeAs-122 phase has also been shown to exhibit superconductivity^{14,15}. Therefore, it seems intriguing to know whether it is possible to induce superconductivity by substituting Fe ions with other transition metals, such as Pd which locates just below Ni in the periodic table of elements. In this paper, we report the successful fabrication of new superconductors in $\text{SrFe}_{2-x}\text{Pd}_x\text{As}_2$. X-ray diffraction pattern (XRD), resistivity, DC magnetic susceptibility, upper critical field as well as the phase diagram have been determined in the system of $\text{SrFe}_{2-x}\text{Pd}_x\text{As}_2$.

We employed a two-step solid state reaction method to synthesize the $\text{SrFe}_{2-x}\text{Pd}_x\text{As}_2$ samples. Firstly, SrAs, FeAs powders were obtained by the chemical reaction method with Sr pieces, Fe powders (purity 99.99%), and As grains. Then they were mixed together in the formula $\text{SrFe}_{2-x}\text{Pd}_x\text{As}_2$, ground and pressed into a pellet shape. All the weighing, mixing and pressing procedures were performed in a glove box with a protective argon atmosphere (both H_2O and O_2 are limited below 0.1 ppm). The pellet was sealed in a silica tube with 0.2 bar of Ar gas and followed by heat treatment at 900 °C for 50

hours. Then it was cooled down slowly to room temperature. A repeating of above procedures improves the purity of the samples.

The x-ray diffraction measurement was performed at room temperature using an MXP18A-HF-type diffractometer with $\text{Cu-K}\alpha$ radiation from 10° to 80° with a step of 0.01°. The analysis of x-ray powder diffraction data was done by using the software of Powder-X¹⁶ and the lattice constants were derived by having a general fitting (see below). The DC magnetization measurements were done with a superconducting quantum interference device (Quantum Design, SQUID, MPMS7). The zero-field-cooled magnetization was measured by cooling the sample at zero field to 2 K, then a magnetic field was applied and the data were collected during the warming up process. The field-cooled magnetization data was collected in the warming up process after the sample was cooled down to 2 K at a finite magnetic field. The resistivity measurements were done with a physical property measurement system PPMS-9T (Quantum Design) with the four-probe technique. The current direction was changed for measuring each point in order to remove the contacting thermal power.

In order to have a comprehensive understanding to the evolution induced by the doping effect, we have measured the X-ray diffraction patterns for all samples. The lattice constants of a-axis and c-axis are thus obtained. In Figure 1, we present the x-ray diffraction patterns of $\text{SrFe}_{2-x}\text{Pd}_x\text{As}_2$. It is clear that all main peaks of the samples can be indexed to a tetragonal structure. The peaks marked with asterisks arise from the impurity phase. By fitting the data to the structure calculated with the software Powder-X, we get the lattice constants. In Figure 2, we show a- and c- lattice parameters for the $\text{SrFe}_{2-x}\text{Pd}_x\text{As}_2$ samples. One can see that, by substituting the Pd into the Fe site, the lattice constant a shrinks a bit, while c expands slightly. This tendency is similar to the case of doping the Fe with Ir or Ru in $\text{SrFe}_{2-x}\text{Ir}_x\text{As}_2$ and $\text{BaFe}_{2-x}\text{Ru}_x\text{As}_2$.^{14,15}

In Figure 3, we present the temperature dependence of resistivity for samples $\text{SrFe}_{2-x}\text{Pd}_x\text{As}_2$ with $x = 0, 0.05,$

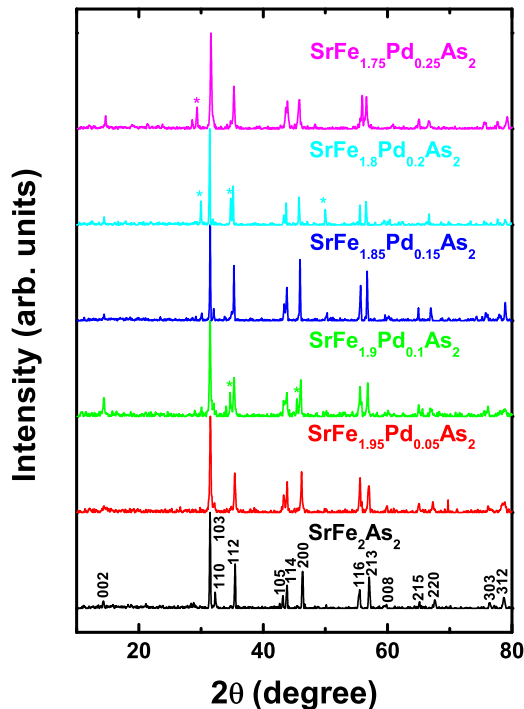


FIG. 1: (Color online) X-ray diffraction patterns for the samples $\text{SrFe}_{2-x}\text{Pd}_x\text{As}_2$. Almost all main peaks can be indexed by a tetragonal structure. The asterisks mark the peaks arising from the impurity phase.

0.1, 0.15, 0.20 and 0.25 respectively. As we can see, the parent phase exhibits a sharp drop of resistivity (resistivity anomaly) at about 215 K. By doping more Pd, the resistivity drop was converted to an uprising. This occurs also in the Co-doped samples. We found that the superconductivity appears in the sample with nominal composition of $x = 0.1$. In the sample of $x = 0.15$, the resistivity anomaly disappeared completely. This sample shows a superconducting transition at about 8.7 K which is determined by a standard method, i.e., using the crossing point of the normal state background and the extrapolation of the transition part with the most steep slope (as shown by the dashed lines in Fig.6). The transition width determined here with the criterion of 10-90 % ρ_n is about 1.2 K. With higher doping level ($x = 0.2$) the transition temperature declines slightly. The superconductivity again disappeared when the doping content x is over 0.25.

In Figure 4, the temperature dependence of the DC magnetization for the sample $\text{SrFe}_{1.85}\text{Pd}_{0.15}\text{As}_2$ was shown. The measurement was carried out under a magnetic field of 20 Oe in zero-field-cooled and field-cooled processes. A clear diamagnetic signal appears below 8.2 K, which corresponds to the middle transition temperature of the resistivity data. A very strong Meiss-

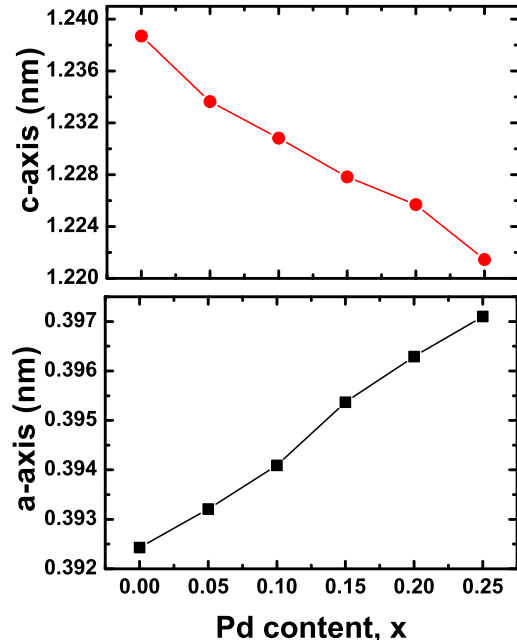


FIG. 2: (Color online) Doping dependence of a-axis lattice constant and c-axis lattice constant. It is clear that the a-axis lattice shrinks, while c-axis lattice expands with Pd substitution. This systematic evolution clearly indicates that the Pd ions have been successfully substituted into the Fe-sites.

ner shielding signal was observed in the low temperature regime, which is similar to the case in $\text{SrFe}_{2-x}\text{Ir}_x\text{As}_2$.

In Figure 5, a phase diagram of $\text{SrFe}_{2-x}\text{Pd}_x\text{As}_2$ within the range of x from 0 to 0.25 was given. Both T_{an} and T_c was defined as temperature of the anomaly in resistivity and the superconductivity transition by resistivity and susceptibility, respectively. Like other samples in FeAs-122 phase, with increasing Pd-doping, the temperature of the resistivity anomaly which may correspond the tetragonal-orthorhombic structural / antiferromagnetic transition is driven down, and the superconductivity emerges at $x = 0.1$, reaching a maximum T_c of 8.7 K at $x=0.15$. The superconducting state disappeared at $x = 0.25$. As we can see, there exists a region in which the antiferromagnetic and superconductivity coexist. This general phase diagram looks very similar to that with Ni-doping.¹² Since Pd locates just below Ni in the periodic table of elements, we would conclude that the superconductivity induced by Pd doping shares the similarity as that of Ni doping. Further measurements on other properties will clarify this point.

In Figure 6 we present the temperature dependence of resistivity broadening induced by using different magnetic fields. Just as many other iron pnictide superconductors, the superconductivity is also very robust against the magnetic field in the present sample although the T_c is only 8.7 K. We used the cri-

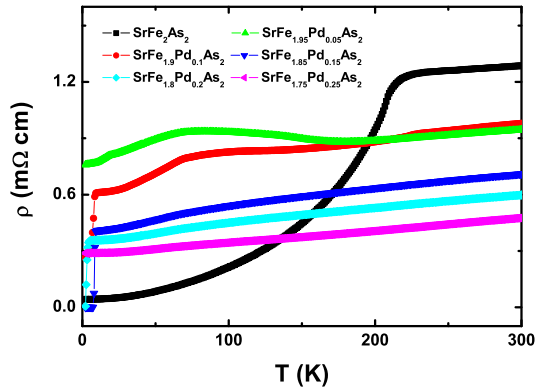


FIG. 3: (Color online) Temperature dependence of resistivity for samples $\text{SrFe}_{2-x}\text{Pd}_x\text{As}_2$ ($x = 0, 0.05, 0.1, 0.15, 0.20$ and 0.25 , respectively). The superconductivity appears already in the sample with $x=0.10$, while the maximum T_c appears at about $x = 0.15$.

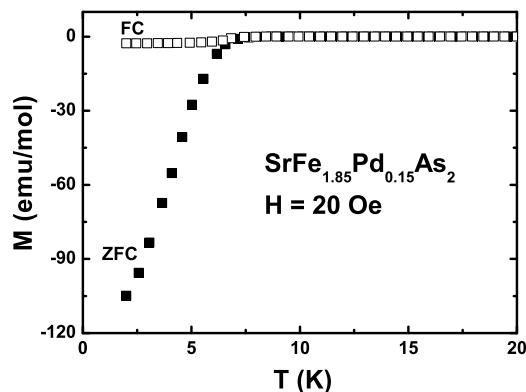


FIG. 4: (Color online) Temperature dependence of DC magnetization for the sample $\text{SrFe}_{1.85}\text{Pd}_{0.15}\text{As}_2$. The measurement was done under a magnetic field of 20 Oe in zero-field-cooled and field-cooled modes. A strong Meissner shielding signal was observed.

terion of $90\%\rho_n$ to determine the upper critical field and show the data in the inset of Figure 6. Surprisingly, regarding the relatively low T_c , a high slope of $-dH_{c2}/dT = 4.2$ T/K can be obtained here. By using the Werthamer-Helfand-Hohenberg (WHH) formula¹⁷ $H_{c2}(0) = -0.69(dH_{c2}/dT)|_{T_c}T_c$, the value of zero temperature upper critical field can be estimated. Taking $T_c = 8.7$ K, we get $H_{c2}(0) \approx 25.1T$ roughly. Because of the low superconducting transition temperature, the present Pd-doped sample has a smaller upper critical field, compared with K-doped¹⁸ and Co-doped samples¹⁹.

The superconductivity mechanism in the FeAs-based superconductors remains unclear yet. One widely per-

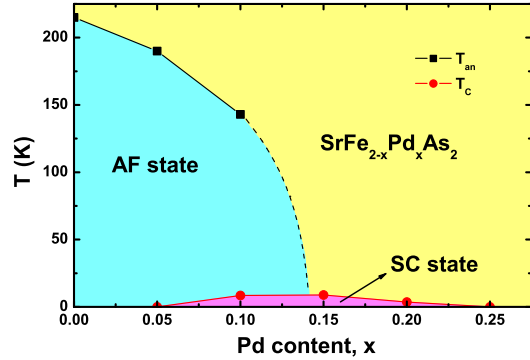


FIG. 5: (Color online) Phase diagram of $\text{SrFe}_{2-x}\text{Pd}_x\text{As}_2$ within the range of $x = 0$ to 0.25 . The temperature of resistivity anomaly represents the upturning point of resistivity which indicates a deviating point from a rough T-linear behavior in the high temperature region. The superconductivity starts to appear at $x \approx 0.05$, reaching a maximum T_c of 8.7 K at $x = 0.15$. The dashed line provides a guide to the eyes for the possible AF order/structural transitions near the optimal doping level.

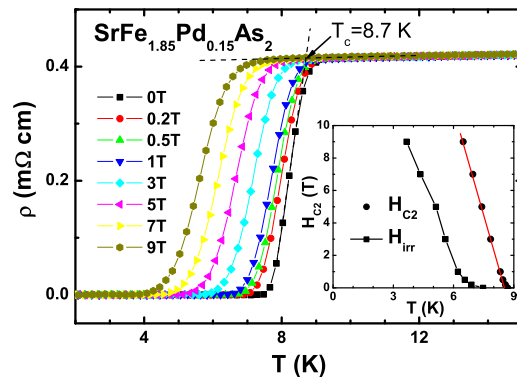


FIG. 6: (Color online) Temperature dependence of resistivity for the sample $\text{SrFe}_{1.85}\text{Pd}_{0.15}\text{As}_2$ at different magnetic fields. The dashed line indicates the extrapolated resistivity in the normal state. One can see that the superconductivity seems to be robust against the magnetic field and shifts slowly to the lower temperatures. The inset gives the upper critical field determined using the criterion of $90\%\rho_n$. A slope of $-dH_{c2}/dT = 4.2$ T/K near T_c is found here. The irreversibility line H_{irr} taking with the criterion of $0.1\%\rho_n$ is also presented in the inset.

ceived picture is that the pairing is established via the inter-pocket scattering of electrons through exchanging the AF spin fluctuations.^{20,21,22,23} By doping electrons or holes into the parent phase, the condition for forming the AF order will be destroyed gradually. Instead the short range AF order will provide a wide spectrum of spin

fluctuations which may play as the media for the pairing between electrons. This picture can certainly give a qualitative explanation to the occurrence of superconductivity here. However, it is still unclear why the superconducting transition temperature varies in doping different elements. For example, the maximum T_c by doping Co, Ni, Ru or Ir can be as high as 24-26 K,^{11,13,14,15} while that by doping Pd in the present case is only about 8.7 K. In addition, in most cases, the substitution to the Fe sites by other transition metal elements in the 1111 phase gives only a rather low superconducting transition temperature compared to the 122 phase. This puzzling point certainly warrants further investigations. Our data here further illustrate that the superconductivity can be easily induced by doping the Fe sites with many other transition metals which are not restricted to the ones with 3d orbital electrons.

In summary, superconductivity has been found in $\text{SrFe}_{1-x}\text{Pd}_x\text{As}_2$ with the maximum $T_c = 8.7$ K. The

phase diagram obtained is quite similar to that by doping Co, Ni, Ru or Ir to the Fe sites. The superconductivity is rather robust against the magnetic field with a slope of $-dH_{c2}/dT = 4.2$ T/K near T_c . Our results clearly indicate that the superconductivity can be easily induced in $(\text{Ba,Sr})\text{Fe}_2\text{As}_2$ by replacing the Fe sites with many different transition metal elements which can be those with 4d- or 5d-orbital electrons.

This work is supported by the Natural Science Foundation of China, the Ministry of Science and Technology of China (973 project: 2006CB601000, 2006CB921802), the Knowledge Innovation Project of Chinese Academy of Sciences (ITSNEM).

References

-
- * Electronic address: hhwen@aphy.iphy.ac.cn
- ¹ Y. Kamihara, T. Watanabe, M. Hirano, and H. Hosono, *J. Am. Chem. Soc.* **130**, 3296 (2008).
 - ² Z. A. Ren, W. Lu, J. Yang, W. Yi, X. L. Shen, Z. C. Li, G. C. Che, X. L. Dong, L. L. Sun, F. Zhou, and Z. X. Zhao, *Chin. Phys. Lett.* **25**, 2215 (2008).
 - ³ C. Wang, L. Li, S. Chi, Z. Zhu, Z. Ren, Y. Li, Y. Wang, X. Lin, Y. Luo, S. Jiang, X. Xu, G. Cao, Z. Xu, *Europhys. Lett.* **83**, 67006 (2008).
 - ⁴ X. Zhu, F. Han, P. Cheng, G. Mu, B. Shen, and H. H. Wen, *Europhys. Lett.* **85**, 17011 (2009).
 - ⁵ P. Cheng, B. Shen, G. Mu, X. Zhu, F. Han, B. Zeng, and H. H. Wen, arXiv:cond-mat/0812.1192 (2008), *EPL*, in press.
 - ⁶ H. H. Wen, G. Mu, L. Fang, H. Yang, and X. Zhu, *Europhys. Lett.* **82**, 17009 (2008).
 - ⁷ M. Rotter, M. Tegel, and D. Johrendt, *Phys. Rev. Lett.* **101**, 107006 (2008).
 - ⁸ K. Sasmal, B. Lv, B. Lorenz, A. Guloy, F. Chen, Y. Xue, and C. W. Chu, *Phys. Rev. Lett.* **101**, 107007 (2008).
 - ⁹ N. Ni, S. L. Bud'ko, A. Kreyssig, S. Nandi, G. E. Rustan, A. I. Goldman, S. Gupta, J. D. Corbett, A. Kracher, P. C. Canfield, *Phys. Rev. B* **78**, 014507 (2008).
 - ¹⁰ H. Luo, Z. Wang, H. Yang, P. Cheng, X. Zhu, H. H. Wen, *Supercond. Sci. Technol.* **21**, 125014 (2008).
 - ¹¹ A. S. Sefat, R. Jin, M. A. McGuire, B. C. Sales, D. J. Singh, and D. Mandrus, *Phys. Rev. Lett.* **101**, 117004 (2008).
 - ¹² Y. K. Li, X. Lin, Z. W. Zhu, H. Chen, C. Wang, L. J. Li, Y. K. Luo, M. He, Q. Tao, H. Y. Li, G. H. Cao, Z. A. Xu, *Phys. Rev. B* **79**, 054521 (2009).
 - ¹³ L. J. Li, Q. B. Wang, Y. K. Luo, H. Chen, Q. Tao, Y. K. Li, X. Lin, M. He, Z. W. Zhu, G. H. Cao, and Z. A. Xu, arXiv:cond-mat/0809.2009 (2008).
 - ¹⁴ S. Paulraj, S. Sharma, A. Bharathi, A. T. Satya, S. Chandra, Y. Hariharan, and C. S. Sundar, arXiv:cond-mat/0902.2728 (2009).
 - ¹⁵ F. Han, X. Zhu, Y. Jia, L. Fang, P. Cheng, H. Luo, B. Shen, H. H. Wen, arXiv:cond-mat/0902.3957 (2009).
 - ¹⁶ C. Dong, *J. Appl. Cryst.* **32**, 838 (1999).
 - ¹⁷ N. R. Werthamer, E. Helfand, P. C. Hohenberg, *Phys. Rev.* **147**, 295 (1966).
 - ¹⁸ Z. S. Wang, H. Q. Luo, C. Ren, H. H. Wen, *Phys. Rev. B* **78**, 140501(R) (2008).
 - ¹⁹ Y. J. Jo, J. Jaroszynski, A. Yamamoto, A. Gurevich, S. C. Riggs, G. S. Boebinger, D. Larbalastier, H. H. Wen, N. D. Zhigadlo, S. Katrych, Z. Bukowski, J. Karpinski, R. H. Liu, H. Chen, X. H. Chen, L. Balicas, arXiv:cond-mat/0902.0532 (2009).
 - ²⁰ I. I. Mazin, D. J. Singh, M. D. Johannes, M. H. Du, *Phys. Rev. Lett.* **101**, 057003 (2008).
 - ²¹ K. Kuroki, S. Onari, R. Arita, H. Usui, Y. Tanaka, H. Kontani, H. Aoki, *Phys. Rev. Lett.* **101**, 087004 (2008).
 - ²² F. Wang, H. Zhai, Y. Ran, A. Vishwanath, D. H. Lee, *Phys. Rev. Lett.* **102**, 047005 (2009).
 - ²³ Q. Han, Y. Chen, Z. D. Wang, *EPL*, **82**, 37007 (2008).